DAMAGE DEVELOPMENT ANALYSIS BASED ON STRAIN ENERGY RELEASE RATE FOR 3-D WOVEN COMPOSITE

Risa Tanaka [1], and Naoyuki Watanabe [2],

[1] Dept. of Aerospace Engineering, Graduate school of Tokyo Metropolitan University
[2] Dept. of Aerospace Engineering, Tokyo Metropolitan University
[1, 2] JP-1910065 Tokyo, Japan
wata@aswat1.cc.tmit.ac.jp

ABSTRACT

3-D FEM simulation of the progressive failure process of 3-D orthogonal interlocked fabric composites including the thermal effects calculated by the homogenization method was carried out in order to establish this present analytical method as one of the damage development simulations. Hashin's criterion was utilized in order to predict the crack onset whereas the strain energy criterion with the crack closure method was adopted for the crack propagation. And transverse cracks occurred in the in-plain fiber tows were simulated with Node Separation Method. Through the simulation, the detailed behaviours of the failures were clarified. With considering the total number of the cracks and the sequence and timing of the whole failure process, it can be concluded that this present method was established sufficiently and efficiently as one of the damage development analyses.

1. INTRODUCTION

Fiber-reinforced composite materials have many advantages and are frequently used in a wide variety of application. Therefore it is quite important to evaluate their failure mechanism analytically and experimentally. Methods of damage development analyses for various types of them such as 3-D woven composite have not been established sufficiently because it is quite difficult to simulate the failure propagation.

Nagai et al. established the simple stress analysis and approximated strength method through expressing the mechanical structure for the woven structure three-dimensionally [1]. Cox et al. executed the finite element analysis with adopting the binary model which can consider the undulation of the fiber tow in order to obtain the stiffness of the 3-D composite with out-of-plane fiber tow arranged orthogonally or in various angle [2]. A FEM simulation of failure process of 3-D orthogonal interlocked fabric composite was executed by Mibayashi including the thermal residual stresses after the curing process [3]. The deformations and stresses were calculated by the homogeneous method and Tsai-Wu criterion was utilized as a failure law over the whole failure process in order to judge whether the elements were failed or not. The simulation of the failure process was carried out until the rupture of the fiber while considering the occurrence of the transverse cracks, and finally the failure mechanism was evaluated. Also a FEM simulation of 2-D plain woven CF/Epoxy laminates was executed in the same manner including both of the transverse cracks in the fiber tows and delaminations between them by Tanaka [4]. However, it is well known that the energy criterion should be adopted to predict crack propagation from the viewpoint of the fracture mechanism except for the crack onset.

Therefore, our objective in this study is to newly establish an effective and accurate method of damage development analysis. This simulation is applied to the 3-D orthogonal interlocked fabric composite with both of Hashin's and energy criteria in

order to estimate the failures. The former one is for the transverse cracks onset whereas the latter one together with crack closure method is applied for the crack propagation.

2. Theory

2.1 Homogenization method

The homogenization method is a rigorous analytical method to the system composed of a large amount of periodic microstructures, which is microscopically heterogeneous but can be regarded as macroscopically homogeneous. In the thermal-elasticity problem such as composite materials, this method which can define the precise boundary condition to them gives considerably accurate equivalent elastic constants and distributions for highly and locally changing stresses in the small base cell that is a minimum unit [5].

The stress-strain expression including the thermal effects and the strain-displacement relation obtained by the assumption of the infinitesimal deformation is given as following with E_{ijkl}^{ε} indicating elasticity tensor.

$$\sigma_{ij}^{\varepsilon} = E_{ijkl}^{\varepsilon}\left[\frac{1}{2}\left(\frac{\partial u_k^{e}}{\partial x_l}+\frac{\partial u_l^{\varepsilon}}{\partial x_k}\right)-\alpha_{kl}^{\varepsilon}\Delta T\right] \tag{2.1}$$

where $\alpha_{kl}^{\varepsilon}$ and ΔT are thermal expansion coefficients of the body and the temperature difference between the current state and the reference one, respectively. Besides, superscript ε means a function of the total region including the micro structures in the remainder of this paper.

The solution of the above thermo-elasticity problem can be obtained by the weak form based on the principle of virtual work with defining the real and virtual displacement components as $u_i^{\varepsilon}(x)$ and $v_i(x,y)$, respectively.

$$\int_{\Omega^{\varepsilon}} E_{ijkl}^{\varepsilon}\left(\frac{\partial u_k^{\varepsilon}}{\partial x_l}-\alpha_{kl}^{\varepsilon}\Delta T\right)\frac{\partial v_i}{\partial x_j}d\Omega=\int_{\Omega^{\varepsilon}} f_i^{\varepsilon}v_i d\Omega+\int_{\Gamma_t} t_i v_i d\Gamma \tag{2.2}$$

where f_i and t_i are a body forces and surface tractions, respectively. Eqs. (2.2) is assumed to satisfy the predicted geometrical boundary condition. The rigorous displacement and stress field are assumed to obey asymptotic expansion with respect to ε. The solutions of thermo-elasticity problem are obtained as follows [9].

$$u^{\varepsilon}(x)=u^{0}(x,y)+\varepsilon u^{1}(x,y), \quad u_i^{0}(x,y)=u_i^{0}(x) \tag{2.3), (2.4}$$

$$u_i^{l}(y)=-\chi_i^{kl}(y)\frac{\partial u_k^{0}(x,y)}{\partial x_l}-\Psi_i(y)\Delta T\,, \quad \sigma^{\varepsilon}(x)=\sigma^{0}(x,y) \tag{2.5), (2.6}$$

$$\sigma_{ij}^{0}(x,y)=\left(E_{ijkl}(x,y)-E_{ijpm}(x,y)\frac{\partial \chi_p^{kl}(x,y)}{\partial y_m}\right)\frac{\partial u_k^{0}(x)}{\partial x_l}-E_{ijkl}(x,y)\frac{\partial \Psi_k(x,y)}{\partial y_l}-E_{ijkl}(x,y)\alpha_k\Delta T \tag{2.7}$$

where χ_i^{kl} and Ψ that are the characteristic displacement tensor and thermal ones can be computed by the following equations.

$$\int_{¥}\left(E_{ijkl}(x,y)-E_{ijpm}\frac{\partial\chi_p^{kl}}{\partial y_m}\right)\frac{\partial v_i(y)}{\partial y_j}dY=0 \tag{2.8}$$

$$\int_{¥}\left(E_{ijkl}\alpha_{kl}^{\varepsilon}\Delta T-\frac{\partial\Psi_k}{\partial y_l}\right)\frac{\partial v_i}{\partial y_i}dY=0 \tag{2.9}$$

In the three-dimensional formulation, the six sets of problem relating to $\chi_i^{kl}(k,l=1,2,3)$ must be obtained considering its symmetry. Consequently, macroscopic homogenized elastic constants E_{ijkl}^{ε} are defined as.

$$E_{ijkl}^{0}=\frac{1}{|Y|}\int_{¥}\left(E_{ijkl}-E_{ijpm}\frac{\partial\chi_p^{kl}}{\partial y_m}\right)dY \tag{2.10}$$

and u_i^0 is the macroscopic deformation when the body is assumed to be macroscopically homogeneous with above elastic constants E_{ijkl}^0 as

$$\int_{\Omega}E_{ijkl}^{0}\left(\frac{\partial u_k^0}{\partial x_l}-\alpha_{kl}^{\varepsilon}\Delta T\right)\frac{\partial v_i(x)}{\partial x_j}d\Omega=\int_{\Omega}\tau_{ij}(x)\frac{\partial v_i(x)}{\partial x_j}d\Omega+\int_{\Omega}\sigma_{ij}^{t}(x)\frac{\partial v_i(x)}{\partial x_j}d\Omega+\int_{\Omega}b_i(x)v_i(x)d\Omega+\int_{\Gamma_t}t_i(x)v_i(x)d\Gamma \tag{2.11}$$

where

$$\tau_{ij}(x)=\frac{1}{|Y|}\int_{¥}E_{ijkl}\frac{\partial\Psi_k}{\partial y_l}dY,\quad \sigma_{ij}^{t}(x)=\frac{1}{|Y|}\int_{¥}E_{ijkl}\alpha_{kl}\Delta TdY \tag{2.12), (2.13}$$

$$b_i(x)=\frac{1}{|Y|}\int_{¥}f_i dY \tag{2.14}$$

where eqs. (2.12) and (2.13) are the terms expressing the micro- and macroscopic thermal deformation effect.

As shown above, the macro- and microscopic problems are not coupled, i.e. the characteristic displacement χ_i^{kl} and Ψ can be computed within the base cell by solving eqs. (2.8) and (2.9), and the homogenized elastic constants are calculated by using eq. (2.10), which does not depend on the macroscopic deformation u_i^0. The microscopic problems only need to be solved once since the body has a uniform cell structure in the whole domain in this analysis.

2.2 Stress criterion

Hashin's criterion [6] that is based on the stress interaction is adopted for predicting the crack onset. Failure modes are categorized as, tension fiber mode, compressive fiber mode, tensile matrix mode, or compressive matrix mode. Here, only the matrix mode is applied to this study since Maximum stress criterion is adopted for estimating the rupture of the fiber. The matrix mode can be written as followings:

$$\sigma_{22}+\sigma_{33}>0 \quad \text{then,} \quad \frac{1}{F_{Lc}^2}(\sigma_{22}+\sigma_{33})^2+\frac{1}{S_{Lc}^2}(\sigma_{23}^2-\sigma_{22}\sigma_{33})^2+\frac{1}{S_{Lt}^2}(\sigma_{12}^2+\sigma_{13}^2)=1 \tag{2.15}$$

Otherwise,

$$\frac{1}{F_{Lc}}\left[\left(\frac{F_{22}}{2S_{Lc}}\right)^2-1\right](\sigma_{22}+\sigma_{33})+\frac{1}{4S_{Lc}^2}(\sigma_{22}+\sigma_{33})^2+\frac{1}{S_{Lc}^2}\left(\sigma_{23}^2-\sigma_{22}\sigma_{33}\right)^2+\frac{1}{S_{Lt}^2}\left(\sigma_{12}^2+\sigma_{13}^2\right)=1 \quad (2.16)$$

2.3 Strain energy release rate and crack closure method [7]

The strain energy release rate is adopted and applied to the energy criterion for the estimating the crack propagation. The strain energy release rate G can be obtained by the crack closure method developed from crack closure integral by Irwin [8]. According to Irwin, the energy can be calculated as a work that is necessary to close the crack into the reference length [9]. As for the fracture criterion, the mixed mode of all mode I, II and III is supposed by given the following equation, where G_{IC}, G_{IIC}, and G_{IIIC} are the critical strain energy release rates in each mode.

$$\left(\frac{G_I}{G_{IC}}\right)^2+\left(\frac{G_{II}}{G_{IIC}}\right)^2+\left(\frac{G_{III}}{G_{IIIC}}\right)^2\geq 1 \quad (2.17)$$

3. ANALYTICAL PROCEDURE

3.1 Model for simulation

Since the structure of the three dimensional orthogonal interlocked fabric composite is considerably simple, it is one of suitable composites a model for the present analysis in the first trial and Figure 1 (a) shows the photo of the cross sectional view. The in- and out-of-plane tows lay as seen Figure 1 (a) and the periodic micro structure can be seen inside the pink square. Therefore, the homogenization method can be adopted for calculating the stress and deformation. The minimum periodic region is defined as the base cell in the method and given as Figure 1 (b) in which each fiber tows and epoxy region are arranged as shown. The size of the base cell is $3.00\times 3.00\times 0.596 \quad mm$.

T300, T900 and Epoxy 828 are adopted for the in-, out-of-plane fibers and for the resin and the material properties of them without T900 are indicated in Table 1. The Young's modulus E_L of T900 is 294 GPa and the other properties of it are supposed to be those of T300 for the simplicity. The fiber volume fraction within the in- and out-of-plane fiber tows are assumed to be 54.6 and 54.4. The material properties of the tows are calculated with each V_f by supposing that the fibers are placed in hexagonal array and using the homogenization method and they are listed in Table 2.

Table 3 illustrates the six strength parameters $(F_{Lt}, T_{Lc}, F_{Tt}, F_{Tc}, S_{Lt}, S_{Tt})$ of every fiber tow for the stress criterion and these values are refereed from the strength ones of CF/Epoxy with the fiber fracture volume 60% [10]. Consequently, the values of fracture toughness in G_{IC} and G_{IIC} for the energy criterion are defined as 140 and 500 N/m. They are modified on the basis of those of T300/Epoxy unidirectional composite materials according to Kageyama [11]. It is too difficult to estimate G_{IIIC} because of the experimental difficulty, however, the effect of mode III can be regarded quite slight since mode I is dominant in this problem. Therefore it does not matter that G_{IIIC} is supposed to be the same value of G_{IIC}.

20 nodes solid elements are adopted and the number of the elements and nodes of the base cell are 4840 and 22241. The base cell is made with Patran (MSB Co.Ltd) and it can be simulated with HP xw8000 workstation through our originally developed program to include the homogenization method. Patran is also adopted to show deformations or stress distributions of the calculated results.

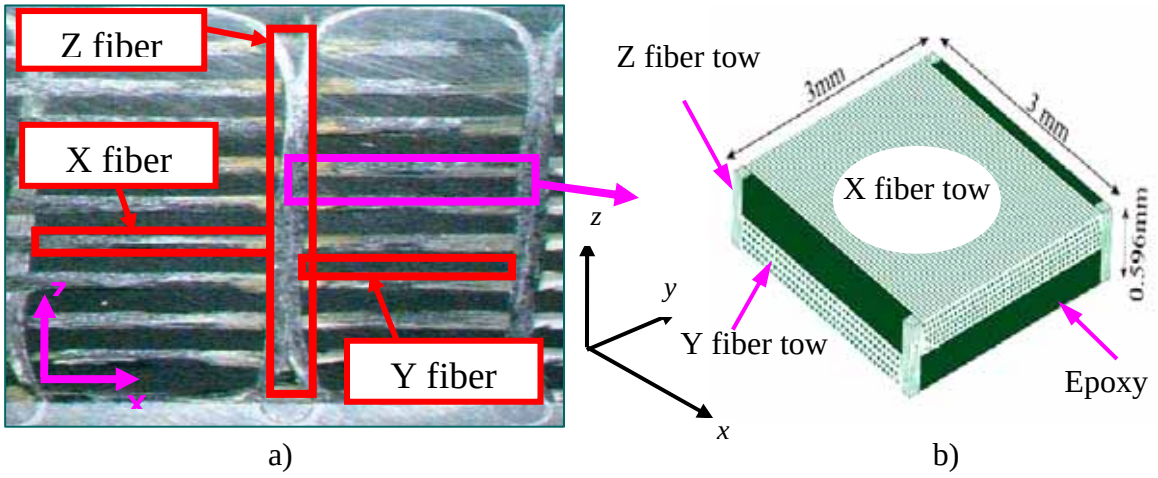

a) b)

Figure 1: a) Photo of the cross sectional view and b) base cell of three dimensional orthogonal interlocked fabric composite

3.2 Algorithm of simulation

In the analysis, the extended homogenization method with including the thermal effect is applied to the base cell. The transverse cracks are only considered as a failure type and supposed to occur symmetrically on the x-y plane. In order to simulate transverse cracks in the in-plane fiber tows, Node separation method, 'NSM' is adopted. In this method, the common nodes on the interface between the focused element and the adjacent one on the boundary are changed into double nodes when both of these elements are judged to be failed or when the cracks are regarded to propagate on the basis of the energy criterion. The algorithm over the whole simulation is as follows:

STEP 1: Homogenized elastic constants and distribution of thermal residual stresses are calculated by assuming that a temperature drop during the curing process is 130 K.

STEP 2: The base cell is subjected to uni-axial tensile load parallel to the x-axis.

STEP 3: After averaging obtained stress components in each finite element, the crack onset is predicted as a candidate on the basis of Hashin's criterion.

Let us consider a situation as an example that there are two crack candidates (a) and (b) with a length of an element as shown red lines in Figure 2 I).

STEP 4: Let each candidate extend in the crack closure method process in order to examine which candidate can be progressed with the lower applied stress while the other crack is closed like in Figure 2 II). After comparing the two crack candidates, only the one with the lower stress is picked up and

simulated whereas the other one is closed here. Let us suppose that it is the crack candidate (b), and then the situation becomes like Figure 2 II).

STEP 5: As for the crack propagation, let an existing crack, i.e. the crack (b), extend in order to know whether it can be developed or not. The red line in Figure 2 III) indicates the opening part of this crack. Also the crack candidate (a) is made extend for a comparison while the crack (b) exists as the green line in Figure 2 II). After that, either the crack or crack candidate is chosen and simulated.

Here, the whole process from STEP 1 to 5 is called as the one iteration. The analysis was executed with repeating this iteration until a X fiber is expected to rupture judged with Maximum stress criterion since the structure was assumed to suffer the ultimate failure if the fiber breakage occurs in the X fiber tow. In this procedure, the thermal residual stresses due to the temperature drop during the curing process are also calculated every repeating time since they are changing with the new occurring failures simulated with NSM.

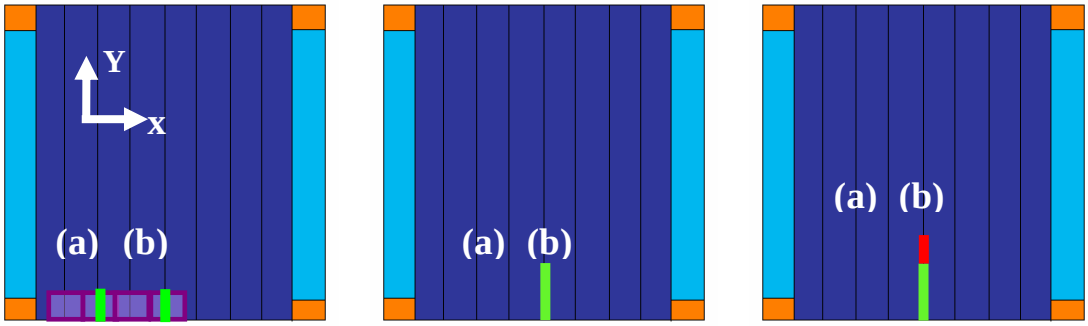

I) II) III)

Figure 2: Algorithm of simulation

Table 1: Material Properties of Carbon Fibers and Epoxy828

	E_L (GPa)	E_T (GPa)	G_{LT} (GPa)	G_{TT} (GPa)	ν_{LT}	$\alpha_L \times 10^{-8}$ $(1/T)$	$\alpha_T \times 10^{-5}$ $(1/T)$
T300	230	18.6	42.1	6.60	0.32	-0.78	0.81
Epoxy 828	3.5	3.5	1.3	1.3	0.35	645	6.45

Table 2: Material properties of each fiber tow

	V_f $(\%)$	E_L (GPa)	E_T (GPa)	G_{LT} (GPa)	G_{TT} (GPa)	ν_{LT}	$\alpha_L \times 10^{-8}$ $(1/T)$	$\alpha_T \times 10^{-5}$ $(1/T)$
X and Y	54.6	127.12	8.09	3.89	2.68	0.345	6.04	4.18
Z	46	148.72	7.53	3.46	2.48	0.348	0.81	4.56

Table 3: Strength of Fiber tow (volume of fiber: $V_f = 0.6$) [GPa]

F_{Lt}	F_{Lc}	F_{Tt}	F_{Tc}	S_{Lt}	S_{Tt}
1.48	1.49	0.08	0.28	0.093	0.093

4. RESULTS

4.1 Distribution of thermal residual stress

In the analysis including the thermal effect, an accurate distribution of the stresses in the base cell is obtained through calculating with the homogenization method by considering periodic boundary conditions. The distribution of thermal stress σ_x^T is shown in Figure 5 that is the lower left quarter part of the base cell. Since Thermal expansion coefficient (TEC) of each fiber tow in the fiber direction is much smaller than that in transverse to fiber direction and that of the Epoxy, the compressive σ_x^T occurs in the X fiber tow whereas the tensile stress exists in the Y fiber tow and the Epoxy region. The tensile stress concentration occurs near the boundary of all, whereas the negative is on the Y fiber tow that is contiguous to the Epoxy region. These results can be reasonable because the thermal residual stress occurs due to the mismatch of TEC.

4.2 Failure process

The failure process of the damage development analysis with Hashin's criterion and the strain energy release rate are as follows. Figure 3 shows how the applied stress has varied at the every iteration.

Up to the 4th iteration, the transverse crack candidates are supposed to initiate with only a length of element caused by the thermal effect. They are illustrated as X-b, Y-c, X-c, and Y-b in Figure 4 a) and b), where the X and Y fiber tow are schematically expressed.

And then, with the applied stress of 117 and 197 MPa, the transverse crack candidates are only assumed to initiate in the Y and X fiber tow as indicated as Y-d and X-a in Figure 4 a) and b). All these cracks are still closed because they are not satisfied with the energy criterion. Since Y-c candidate satisfies also the energy criterion with 273 MPa at the 8th iteration, it initiates and begins to propagate exact in the center of the Y fiber tow as shown in Figure 6, where only this tow is shown. It is natural that the crack occurs first in the Y fiber tow because of the applied stress parallel to the x direction and the thermal residual stress. Figure 7 gives the distribution of σ_x and the effect by the crack occurrence can be seen around and adjacent to that crack and the tensile stress concentration is observed in the region around the Z fiber tow. After that, with the higher stress, the existing crack is propagating and finally penetrates in the length direction with the stress 312 MPa at the 22nd iteration.

Next, with the applied stress 343 MPa at 23rd iteration, the other cracks as illustrated as Y-a in Figure 4 initiate and propagate in the Y fiber tow and then penetrate completely as shown Figure 8. Thirdly, with the applied stress 605 MPa at 36th iteration, the last cracks as given as Y-d in Figure 4 initiate in the Y fiber tow and penetrate at 42nd as shown in Figure 9. Under the crack process from the onset to penetration, the applied stress has decreased obviously, which means that the cracks start and penetrate

at the same time. Since it is quite well known from the experiments that cracks start and penetrate at the same time in the usual laminates, this fact is one of a sustainable reasons of the present simulation.

After that, until the end of the process, no more cracks initiate in the Y fiber tow, but only one crack indicated as X-b in Figure 4 a) starts precisely at the center in the X fiber tow. However, it has propagated quite slightly until the X fiber is supposed to rupture with the applied stress 669 MPa at 48th iteration. Figure 10 shows the distribution of σ_x at that time and also the effect of the crack in the X fiber tow can be observed. And the rupture occurs as indicated in the two green circles in Figure 9 on the surface of the X fiber tow where the occurring transverse cracks in the Y fiber tow affected most directly. On the whole, the first crack occurs at the precise center and the rest of them near the edge in the Y fiber tow. The Z fiber tows are arranged at each corner and they lead the stress concentration there so that these places can be reasonable.

Therefore, with considering the alteration of the stress distributions, the total number of the cracks, and the sequence and timing of the crack onset and propagation over the whole process, it can be concluded that the present analysis including the failures simulated with NSM was carried out precisely and that the algorithm of the strain energy criterion on the basis of the crack closure method was sufficiently established.

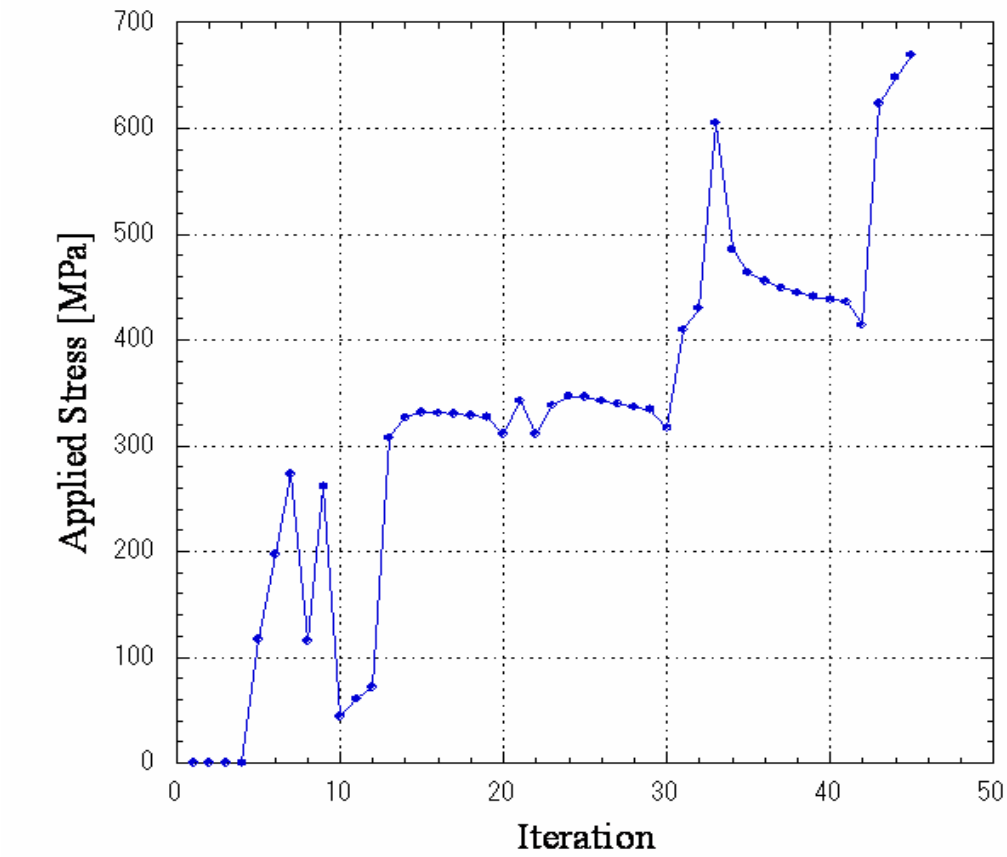

Figure 3: Applied stress on each iteration

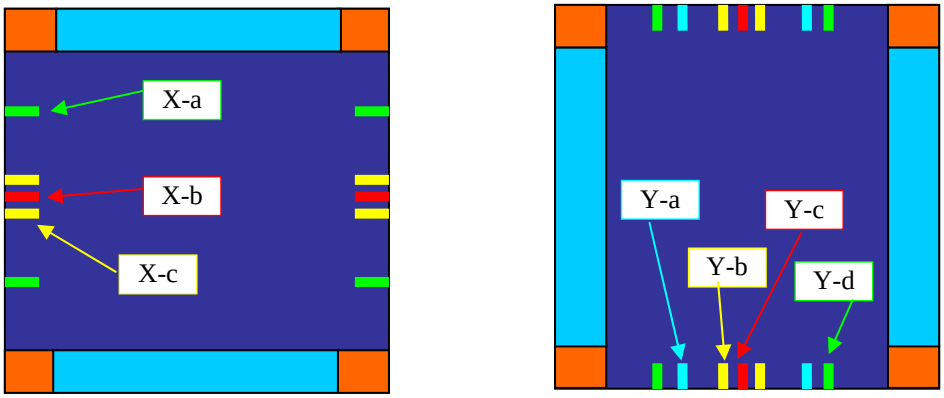

a) b)

Figure 4: Simple views of a) X and b) Y fiber tow

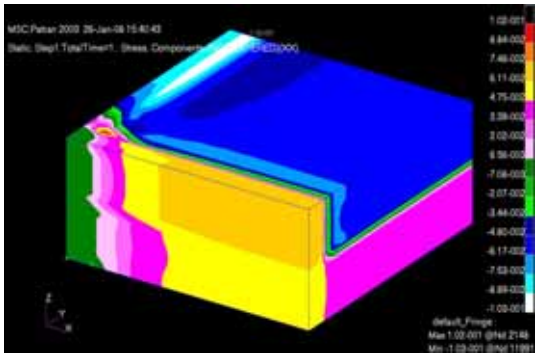

Figure 5: Thermal stress σ_x

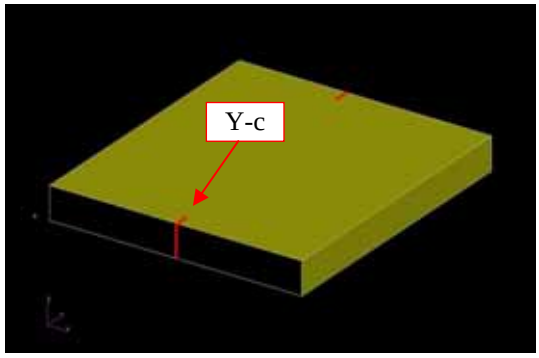

Figure 6: Crack occurrence at 273 MPa

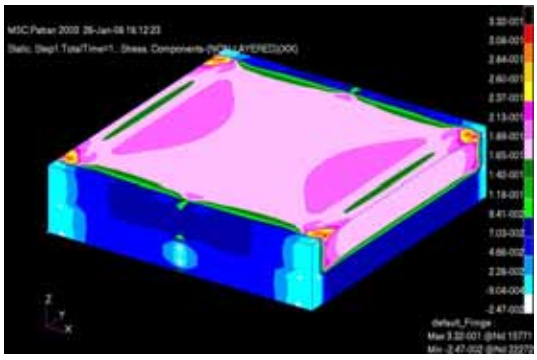

Figure 7: σ_x at 273 MPa

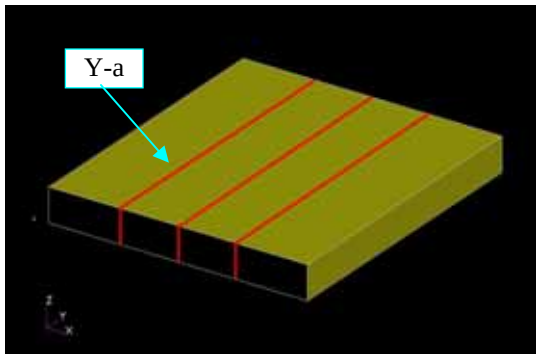

Figure 8: Crack occurrence at 343 MPa

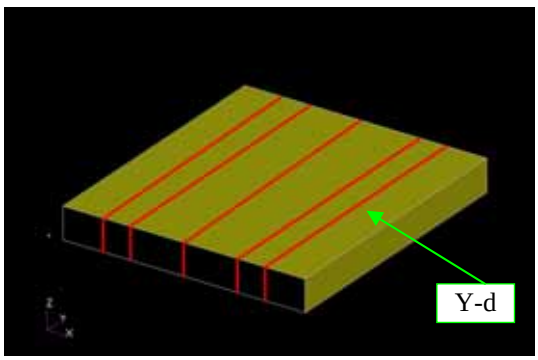

Figure 9: Crack occurrence at 609 MPa

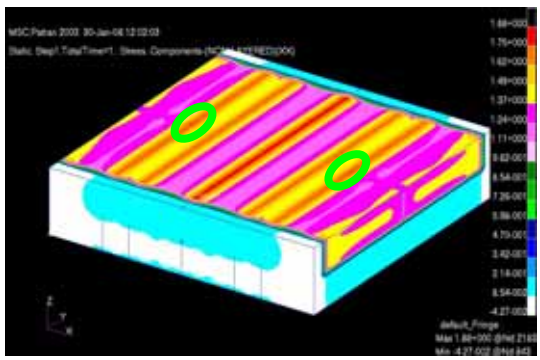

Figure 10: σ_x at 669 MPa

4. CONCLUSIONS

Damage development FEM simulation for 3-D orthogonal interlocked fabric composites with considering the thermal residual stresses calculated by the homogenization method was carried out on the basis both of stress and energy criterion for the transverse crack onset and propagation, respectively. From the simulation, the behaviours of the transverse cracks could be clarified as follows:

Firstly, the transverse cracks are supposed to initiate only by the very high thermal stress. One transverse crack initiates precisely at the centre in the Y fiber tow, and then five cracks totally occurred in it to the end of the simulation whereas only one crack began in the X fiber tow. The first and second occurring cracks in the Y fiber tow penetrated with the little higher applied stress than its onset and the last ones penetrated at the same time of its own onset. The crack in the X fiber tow had propagated only slightly, until the X fiber was supposed to rupture.

Therefore it can be concluded with evaluating the alteration of the total number of the cracks, and the sequence and timing of the crack onset and propagation over the whole process that this present method with added the algorithm of strain energy release rate is established sufficiently and efficiently as one of the damage development simulations.

5. REFERENCES

1- Nagai K., Yokoyama A., Maekawa Z., ”Strength Analysis for Three-Dimensional Composite Materials”, *Journal of the Japan society for composite Materials* 22, 1 (1992) 2-9, (in Japanese).

2- Cox N.B., Carter W.C., Fleck N. A., “A Binary Model of Textile Composites – I Formulation”, *Acta Metallurgica et Materialia*, Mater 42, 10 (1994) 3463-3479

3- Mibayashi H., “Damage Development Analysis of 3-D CFRP by Using Node Separation Method”, *Master Thesis of Tokyo Metropolitan Institute of technology*, 2002.

4- Tanaka R., Watanabe N., “FEM simulation of failure process of Woven CF/Epoxy laminates” *ICCM-16*, Kyoto, Japan, 2007 CD-ROM.

5- Watanabe N. and Teranishi K. “Thermal Stress Analysis for AI Honeycomb Sandwich Plates with Very Thin CFRP Faces”, *36th AIAA, Structure*

6- Hashin Z., “Failure Criteria for Unidirectional Fiber Composites,” *Journal of Applied Mechanics*, Vol.47, 1980, pp.329-33

7- Krueger R., ”The Virtual Crack Closure Techniques: History, Approach and Applications”, *ICASE Report* No.2002-10

8- Irwin G.R, ”Fracture”, *Handbuch der Physik* 6, (1958) 551

9- Rybicki E.F., Kanninen M.F., ”A Finite Element Calculation of Stress Intensity Factors By a Modified Crack Closure Integral”, *Eng. Fracture Mech.* 9, (1977) 931-938

10- Naik N. K., and Ganesh V. K., “Failure behavior of plain weave fabric laminates under on-axis uniaxial tensile loading: II - analytical predictions.” *Journal of Composite Materials*, Vol.30, 1996, 1779-1821.

11- Kageyama K., ”Fracture Mechanics (III)”, *Journal of the Japan society for composite Materials* 18, 5 (1992) 208-214, (in Japanese)